

The Fascinating Symmetries of Golden Clusters Containing Two Skeletal Elements [M-2] in the Cluster Nucleus

Enos Masheija Rwantale Kiremire

Correspondence: Enos Masheija Rwantale Kiremire, Department of Chemistry and Biochemistry University of Namibia, Private Bag 13301 Windhoek, Namibia, E-mail: kiremire15@yahoo.com.

Received: December 22, 2016 Accepted: January 31, 2017 Online Published: xx 15, 2016

doi:10.5539/ijc.v9n1p79

URL: <http://dx.doi.org/10.5539/ijc.v9n1p79>

Abstract

The golden clusters containing two skeletal atoms in the cluster nucleus have been analyzed more carefully with the help of the 4n series method. Their shapes can reasonably and readily be predicted by mapping the [M-2] capped clusters of 3 to 13 nuclearity onto Pivoriunas geometrical model. Some of these clusters were historically categorized as being spherically centered.

Keywords: series, spherical, capped, geometrical-model, nuclearity

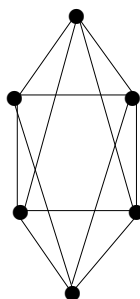
1. Introduction

The shapes of golden clusters have fascinated scientists for some time (Pauling, 1977; Cotton and Wilkinson, 1980; Mingos, 1984, 1987; Steigelmann, et al, 1993; Kappen, et al, 1995a, 1995b; Greenwood and Earnshaw, 1998; Raithby, 1998; Vincente, et al, 1998; Kilmartin, 2010; Kwok-Ming, 2011; Pei, et al, 2011; Yuan, et al, 2013; Sarip, 2013; Puls, 2014; Konishi, 2014). Their geometries were classified as centered, non-centered and exo-attached polyhedral clusters (Konishi, 2014). It has been found that the series method is generally very precise in categorizing and predicting the shapes of clusters such as boranes and their relatives, carbonyl and Zintl clusters (Kiremire, 2016a). The categorization of some golden clusters has been done using skeletal numbers and some of the work published (Kiremire, 2016b, 2016c, 2017). In this paper the emphasis is to closely focus mainly on selected samples of capped golden clusters whose nuclei are comprised of two skeletal elements. The major significance of this paper apart from using the series method to identify the composition of the cluster nucleus is to assign a possible geometrical framework of how other skeletal elements are arranged around the two nuclear skeletal elements to generate the overall skeletal geometry.

2. Results and Discussion

2.1 Background

The series method has evolved to a level where skeletal numbers were assigned to main group and transition metal elements and a few ligands (Kiremire, 2016a, 2016b, 2016c, 2017). The use of skeletal numbers makes it exceedingly easy to categorize and even predict the shapes of some clusters. In many cases, the series method agrees with the literature results and in some gives a more precise categorization and structural prediction. In this work, the skeletal numbers (Kiremire, 2016a, 2016b, 2016c, 2017) will be applied to categorize and characterize a selected sample of golden clusters. It has also been found that a given $k(n)$ parameter defines the shape of the skeletal elements in most cases (k = skeletal linkages of a cluster and n = number of skeletal elements). For instance, $Os_6(CO)_{18}^{2-}$, $k = 6(5) - 18 - 1 = 11$; $Rh_6(CO)_{16}$, $k = 6(4.5) - 16 = 11$; $B_6H_6^{2-}$, $k = 6(2.5) - 3 - 1 = 11$; $SFe_2Ru_3(CO)_{14}^{2-}$, $k = 1(1) + 2(5) + 3(5) - 14 - 1 = 11$; $Se_2Mn_4(CO)_{12}^{2-}$, $k = 2(1) + 4(5.5) - 12 - 1 = 11$; $Co_4P_2(CO)_{10}$, $k = 4(4.5) + 2(1.5) - 10 = 11$; $Ru_6I(CO)_{17}$, $k = 6(5) - 2 - 17 = 11$; and $Re_6(C(CO)_9)^{2-}$, $k = 6(5.5) - 2 - 19 - 1 = 11$. All these clusters are interrelated by the parameter $k(n) = 11(6)$. That is, 11 cluster linkages and 6 skeletal atoms. The characteristic feature of each one of the complexes is the presence of an ideal octahedral skeletal geometry, O_h .



O_h SYMMETRY

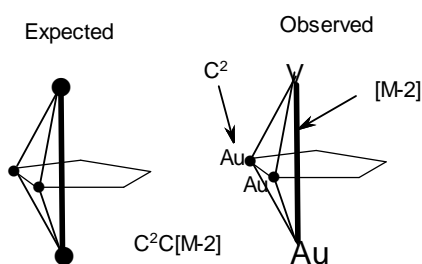
2.2 Categorization of Golden Clusters Using Skeletal Numbers

A golden cluster, like any other cluster can be categorized by using skeletal numbers (Kiremire, 2016, 2017). Let us take a few examples for illustrations.

Ex-1. $(AuL)_3V(CO)_5$

According to series method, the skeletal elements are the providers of the skeletal linkages while the ligands are the consumers of some or all those skeletal linkages. When a cluster comprising of original 'naked' skeletal elements and ligands is formed, the ligands utilize some or all of the skeletal linkages. Then the skeletal linkages remaining $[k(n)]$ are the ones that dictate the symmetry of the cluster as pointed out in the case of the O_h geometry discussed earlier.

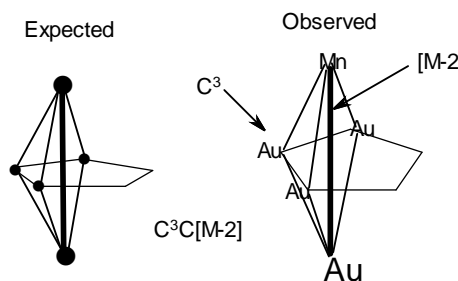
The skeletal number of Au is 3.5 and the ligand L, $k = -1$ (Kiremire, 2016, 2017), hence $[AuL]$ fragment has a k value given by $k = 3.5 - 1 = 2.5$, $V = 6.5$, CO, $k = -1$ (Kiremire, 2016, 2017). It is interesting to note that the fragment $[AuL]$ is isolobal to boron $[B]$. That is, $[AuL] \leftrightarrow [B]$. The $k(n)$ value for the $(AuL)_3V(CO)_5$ cluster is given by $k = 3[2.5] + 1(6.5) - 5(1) = 9$; hence, $k(n) = 9(4)$. For a given series $S = 4n + q$, $k = 2n - q/2$, and $q = 2[2n - k] = 2[2(4) - 9] = 2[-1] = -2$ (Kiremire, 2016c). This gives us the cluster series $S = 4n - 2$, and capping series $C_p = C^1 + C^1 = C^2C[M-2]$. The number of valence electrons is given by $V = 14n - 2 = 14(4) - 2 = 54$. We can verify this value from the formula of the complex, $(AuL)_3V(CO)_5$; $V = 3(11 + 2) + 1(5) + 5(2) = 54$. The symbol $[M-2]$ means that there are 2 skeletal elements which are members of the CLOSO family $S = 4n + 2$ and with $k = 2n - 1 = 2(2) - 1 = 3$. These 2 nuclear skeletal elements will be linked by a triple bond upon which the two capping skeletal elements will be superimposed. This is graphically sketched in F-1.



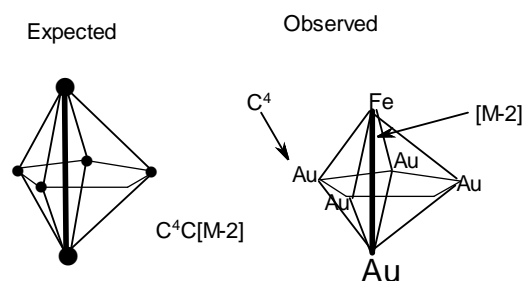
F-1. Graphical representation of the skeletal shape of $(AuL)_3V(CO)_5$

Thus, in this geometrical framework, the nuclear skeletal atoms $[M-2]$ form the vertical axis and the capping skeletal atoms successively occupy the 5 'equatorial' positions around the $[M-2]$ axis. This geometrical framework is adopted from (Pivoriūnas, 2005).

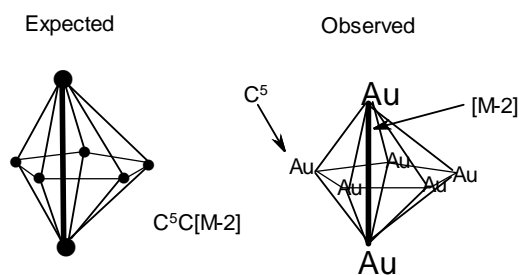
Ex-2. $(AuL)_4Mn(CO)_4^+$; $k = 4[2.5] + 1[5.5] - 4(1) + 0.5 = 12$, $n = 4 + 1 = 5$, $k(n) = 12(5)$. The q value, is calculated in the same way as in Ex-1, $q = 2[2n - k] = 2[2(5) - 12] = 2[-2] = -4$. This gives us $S = 4n - 4$, and $C_p = C^1 + C^2 = C^3C[M-2]$. The number of valence electrons can readily be verified $V = 14n - 4 = 14(5) - 4 = 66$. This agrees with the calculation from the cluster formula $(AuL)_4Mn(CO)_4^+$, $V = (11 + 2)(4) + 7 + 8 - 1 = 66$. Based on the capping symbol $C_p = C^3C[M-2]$, there will be three skeletal capping atoms around the two nuclear skeletal atoms. This is sketched in F-2 and agrees with the observation (Pivoriūnas, 2005).

F-2. Graphical representation of the skeletal shape of $(\text{AuL})_4\text{Mn}(\text{CO})_4^+$

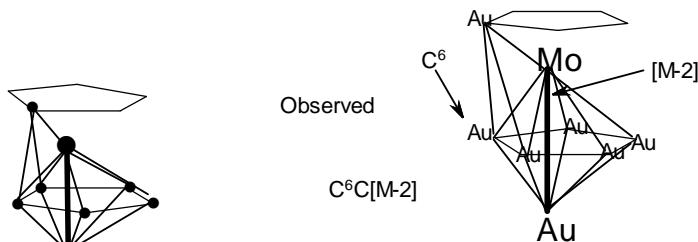
Ex-3. $(\text{AuL})_5\text{Fe}(\text{CO})_3^+$; $k = 5[2.5] + 1(5) - 3 + 0.5 = 15$; $n = 5 + 1 = 6$, $k(n) = 15(6)$. This means we have six skeletal elements. The q value $= 2[2n - k] = 2[2(6) - 15] = 2[-3] = -6$, $S = 4n - 6$, $\text{Cp} = \text{C}^1 + \text{C}^3 = \text{C}^4\text{C}[\text{M}-2]$. The number of valence electrons $V = 14n - 6 = 14(6) - 6 = 78$. Verification from formula, $V = 5(13) + 1(8) + 3(2) - 1 = 78$. Thus, according to the series method and the Pivoriūnas geometrical framework, the $[\text{M}-2]$ skeletal elements will lie along the axis while the remaining 4 skeletal atoms will be distributed around the equatorial positions. This is sketched in F-3 in agreement with the observation (Pivoriūnas, 2005).

F-3. Graphical representation of the skeletal shape of $(\text{AuL})_5\text{Fe}(\text{CO})_3^+$

Ex-4. Au_7L_7^+ , $\text{L} = \text{PPh}_3$; $k = 7(3.5) - 7 + 0.5 = 18$, $k(n) = 18(7)$, $q = 2[2(7) - 18] = 2[-4] = -8$; $S = 4n - 8$, $\text{Cp} = \text{C}^5\text{C}[\text{M}-2]$. Valence electrons $V = 14n - 8 = 14(7) - 8 = 90$. Verification from the formula, $V = 7(11) + 7(2) - 1 = 90$. Clearly, this case will have all the 'equatorial' positions filled up as sketched in F-4. It is not a surprise to that the cluster of that shape is referred to as pentagonal bipyramid (Mingos, 1984; Konishi, 2014) as in $\text{B}_7\text{H}_7^{2-}$ (Greenwood, et al, 1998) with $k(n) = 13(7)$. However, unlike the $\text{B}_7\text{H}_7^{2-}$ cluster, the Au_7L_7^+ complex has a $k(n)$ parameter value of 18(7). This implies that we will expect a different type of cluster bonding.

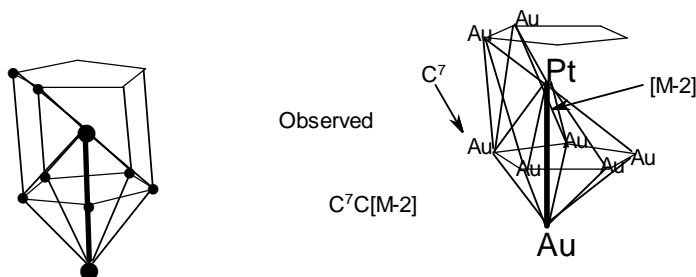
F-4. Graphical representation of the skeletal shape of $(\text{AuL})_7^+$

Ex-5. $(\text{AuL})_7\text{Mo}(\text{CO})_3^+$; following the same procedure as in the above examples, in this case we get, $k(n) = 21(8)$, $S = 4n - 10$, $\text{Cp} = \text{C}^6\text{C}[\text{M}-2]$. Valence electrons $V = 14n - 10 = 14(8) - 10 = 102$. Verification from the formula, $V = 7(13) + 1(6) + 3(2) - 1 = 102$. Here we have 6 capping skeletal elements. The 5 of the capping skeletal elements will complete the first ring of the equatorial arrangement, and the sixth will commence the second ring just above the $[\text{M}-2]$ axis. This sketch is shown in F-5 and agrees with what is observed (Pivoriūnas, 2005).



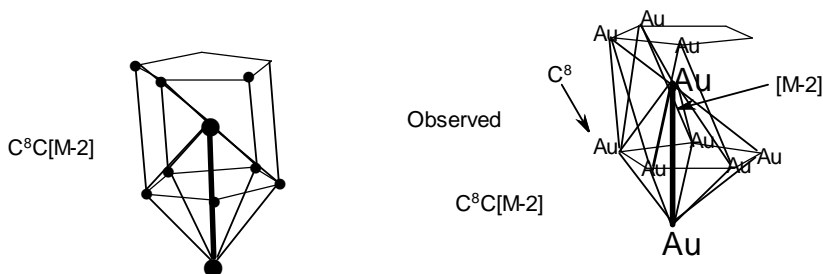
F5. Expected F-5. Graphical representation of the skeletal shape of $(AuL)_7Mo(CO)_3^+$

Ex-6. $(AuL)_8Pt(CO)^{2+}$. Following the same procedure as in the previous examples, $k(n) = 24(9)$, $S = 4n-12$, $Cp = C^7C[M-2]$. The valence electrons $V = 14n-12 = 14(9)-12 = 114$. Verification from formula, $V = 8(13)+1(10)+1(2)-2 = 114$. From the capping symbol, the 7 skeletal elements will be capping around the $[M-2]$ axis. The graphical skeletal shape for the predicted and observed (Gimeno,2008) structures are sketched as shown in F-6.



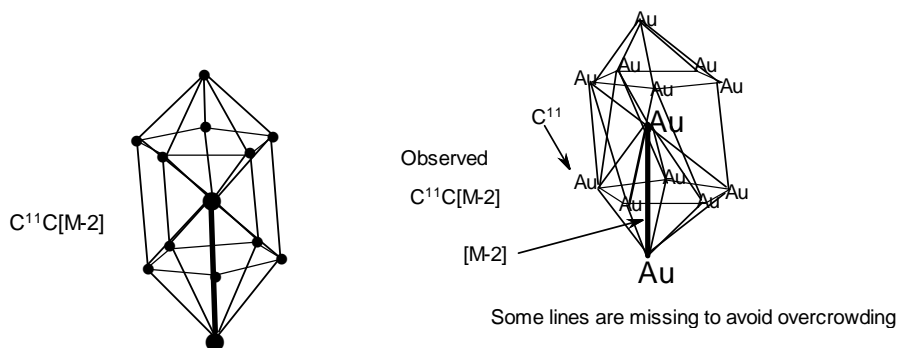
F-6. Expected F-6. Graphical representation of the skeletal shape of $(AuL)_8Pt(CO)^{2+}$

Ex-7. $(AuL)_6(AuCl)_3Pt(CO)$; $k(n) = 27(10)$, $S = 4n-14$, $Cp = C^8C[M-2]$. The valence electrons $V = 14n-14 = 14(10)-14 = 126$. Verification from the formula, $V = 6(13)+3(12)+1(10)+1(2) = 126$. The proposed predicted and observed (Pivoriūnas, 2005) shapes are sketched in F-7.



F-7. Expected F-7. Graphical representation of the skeletal shape of $(Au)_{10}(L)_8^+$

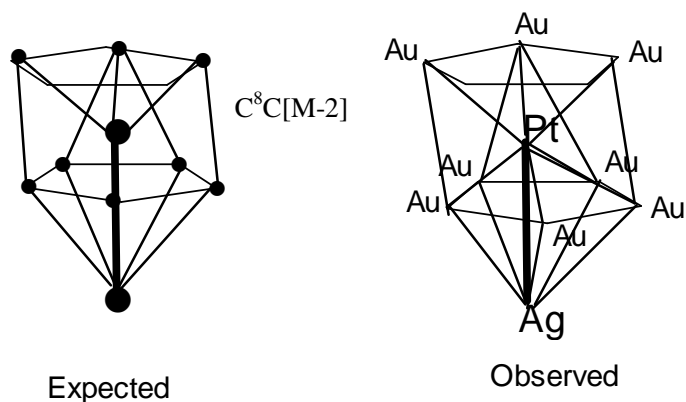
Ex-8. $Au_{13}Cl_2L_{10}^{3+}$; $k(n) = 36(13)$, $S = 4n-20$, $Cp = C^{11}C[M-2]$. The valence electrons $V = 14n-20 = 14(13)-20 = 162$. Verification from formula, $V = 13(11)+2(1)+10(2)-3 = 162$. The proposed skeletal sketch is shown in F-8 and is in agreement with the observation (Konishi, 2014).



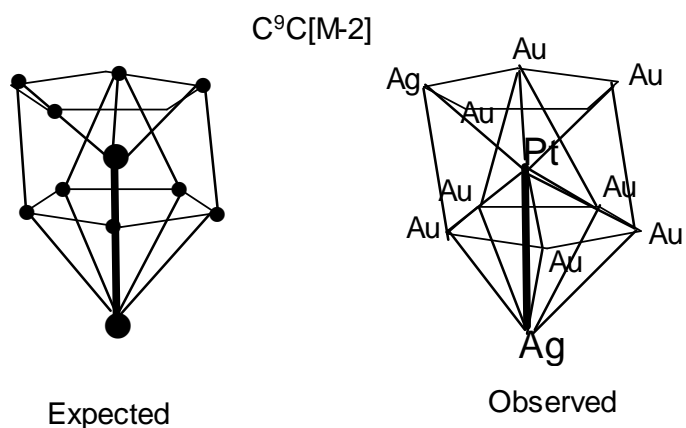
F-8. Expected F-8. Graphical representation of the skeletal shape of $(Au)_{13}Cl_2(L)_{10}^{3+}$

Ex-9. $[\text{Pt}(\text{H})(\text{AgNO}_3)(\text{AuL})_8]^+$

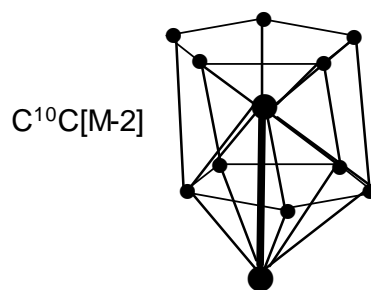
$K = 1[4] + 1[3.5] + 8[2.5] - 0.5 - 0.5 + 0.5 = 27 \rightarrow k(n) = 27(8)$, $4n - 14$, $\text{Cp} = \text{C}8\text{C}[\text{M}-2]$. The valence electrons $V = 14n - 14 = 14(10) - 14 = 126$. Verification from formula, $V = 1[10] + 1(1) + 1(11) + 1(1) + 8(13) - 1 = 126$. The shape will be based on a two-centered skeletal atom nucleus. The other 8 atoms will be capping around $[\text{M}-2]$. This is sketched in F-9 in agreement with the literature (Kappen, 1995b).

F-9. Skeletal sketch of $[\text{Pt}(\text{H})(\text{Ag})(\text{AuL})_8]^+$ Ex-10. $\text{Pt}(\text{H})(\text{AgNO}_3)_2(\text{AuL})_8^+$

$k = 1[4] + 2[3.5] + 8[2.5] - 0.5 + 2(0.5) + 0.5 = 30$; $k(n) = 30(11)$, $S = 4n - 16$, $\text{Cp} = \text{C}1 + \text{C}8 = \text{C}9\text{C}[\text{M}-2]$. The valence electrons $V = 14n - 16 = 14(11) - 16 = 138$. Verification, $V = 1(10) + 1(1) + 2(11) + 1(1) + 8(13) - 1 = 138$. When the nine capped and two centered $[\text{M}-2]$ nucleus cluster are mapped onto the geometrical framework, we get F-10 as has been observed (Kappen, 1995b).

F-10. Skeletal sketch of $[\text{Pt}(\text{H})(\text{Ag})_2(\text{AuL})_8]^{2+}$ Ex-11. $\text{Au}_{12}\text{L}_{10}\text{Cl}_3^+$

$k = 12[3.5] - 10(1) - 1(0.5) + 1.5 = 33$; $k(n) = 33(12)$, $S = 4n - 18$, $\text{Cp} = \text{C}10\text{C}[\text{M}-2]$. The valence electrons $V = 14n - 18 = 14(12) - 18 = 150$. Verification from formula, $V = 12(11) + 10(2) + 1(1) - 3 = 150$. This means that there are 10 capping skeletal atoms while the remaining 2 will be the nucleus, $[\text{M}-2]$. The expected structure is sketched in F-11.



F-11

A selected sample of [M-2] based golden clusters are given in Table 1. Golden clusters have been divided into broad groups such SPHERICAL CLUSTERS and TOROIDAL CLUSTERS (Mingos, 1984). On close analysis with series, the spherical type are found to be those clusters which have a BINUCLEAR INDEX [M-2] (Kiremire, 2016b). Examples include, Au₉L₈⁺, C₇C[M-2], Au₁₁(I)3L₇, C₉C[M-2], and Au₁₃(Cl)₂L₁₀³⁺, C₁₁C[M-2] while the toroidal type are MONONUCLEAR INDEX [M-1] based clusters (Kiremire, 2016b). These include, Au₈L₇²⁺, C₇C[M-1]; Au₉L₈³⁺, C₈C[M-1] and Au₁₀L₆(Cl)₃³⁺, C₉C[M-1].

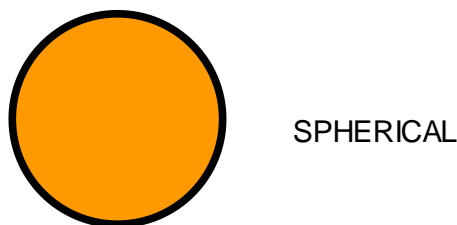
Table 1. Selected [M-2] based Gold Clusters

CLUSTER	k VALUE	k(n)	q VALUE	SERIES	CATEGORY
Mo ₂ (Cp) ₂ (CO) ₄	3	3(2)	2	4n+2	CLOSO[M-2]
Au ₃ L ₃ X ₃	6	6(3)	0	4n+0	C ¹ C[M-2]
(AuL) ₂ Fe(CO) ₄	6	6(3)	0	4n+0	C ¹ C[M-2]
(AuL) ₃ O ⁺	9	9(4)	-2	4n-2	C ² C[M-2]
(AuL) ₃ V(CO) ₅	9	9(4)	-2	4n-2	C ² C[M-2]
(AuL) ₃ Co(CO) ₃	9	9(4)	-2	4n-2	C ² C[M-2]
(AuL) ₃ Fe(CO) ₄ ⁺	9	9(4)	-2	4n-2	C ² C[M-2]
Au ₄ L ₄ I ₂	9	9(4)	-2	4n-2	C ² C[M-2]
Fe ₂ Ir ₂ (CO) ₁₂ (AuL) ⁺	12	12(5)	-4	4n-4	C ³ C[M-2]
(AuL) ₄ Re(CO) ₄ ⁺	12	12(5)	-4	4n-4	C ³ C[M-2]
(AuL) ₄ Co(CO) ₃ ⁺	12	12(5)	-4	4n-4	C ³ C[M-2]
(AuL) ₄ Mn(CO) ₄ ⁺	12	12(5)	-4	4n-4	C ³ C[M-2]
(AuL) ₄ Re(CO) ₄ ⁺	12	12(5)	-4	4n-4	C ³ C[M-2]
(AuL) ₅ Fe(CO) ₃ ⁺	15	15(6)	-6	4n-6	C ⁴ C[M-2]
(AuL) ₅ Mo(CO) ₄ ⁺	15	15(6)	-6	4n-6	C ⁴ C[M-2]
(AuL) ₆ Re(CO) ₃ ⁺	18	18(7)	-8	4n-8	C ⁵ C[M-2]
(AuL) ₆ V(CO) ₄ ⁺	18	18(7)	-8	4n-8	C ⁵ C[M-2]
Au ₇ L ₇ ⁺	18	18(7)	-8	4n-8	C ⁵ C[M-2]
(AuL) ₆ Co(CO) ₂ ⁺	18	18(7)	-8	4n-8	C ⁵ C[M-2]
(AuL) ₆ Mn(CO) ₃ ⁺	18	18(7)	-8	4n-8	C ⁵ C[M-2]
Au ₈ L ₈ ²⁺	21	21(8)	-10	4n-10	C ⁶ C[M-2]
(AuL) ₇ Mo(CO) ₃ ⁺	21	21(8)	-10	4n-10	C ⁶ C[M-2]
(AuL) ₇ Co(CO) ₂ ²⁺	21	21(8)	-10	4n-10	C ⁶ C[M-2]
(AuL) ₈ Pt(CO) ₂ ⁺	24	24(9)	-12	4n-12	C ⁷ C[M-2]
Au ₉ L ₈ ⁺	24	24(9)	-12	4n-12	C ⁷ C[M-2]
(AuL) ₆ (AuCl) ₃ Pt(CO)	27	27(10)	-14	4n-14	C ⁸ C[M-2]
Au ₁₁ L ₇ Cl ₃	30	30(11)	-16	4n-16	C ⁹ C[M-2]
Au ₁₁ L ₇ I ₃	30	30(11)	-16	4n-16	C ⁹ C[M-2]
Au ₁₁ L ₁₀ ³⁺	30	30(11)	-16	4n-16	C ⁹ C[M-2]
Au ₁₃ L ₇ Cl ₅	36	36(13)	-20	4n-20	C ¹¹ C[M-2]
Au ₁₃ Cl ₂ L ₁₀ ³⁺	36	36(13)	-20	4n-20	C ¹¹ C[M-2]
Au ₁₃ L ₁₂ ⁵⁺	36	36(13)	-20	4n-20	C ¹¹ C[M-2]

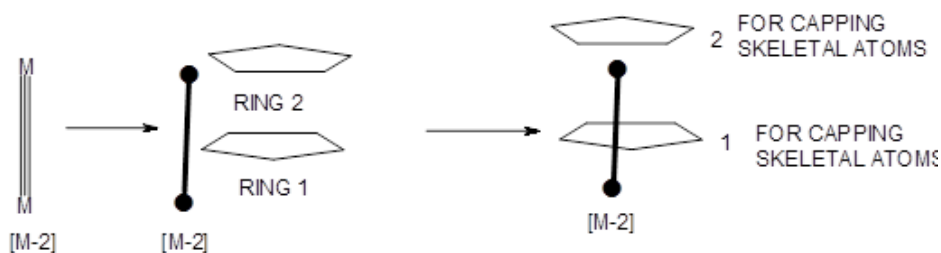
2.3 Hypothetical Model for Predicting the Symmetries of [M-2] Based Golden Clusters

When the clusters in Table 1 are carefully scrutinized, they are found to form a set of capping series based on a closo nucleus comprising of two skeletal elements linked by a triple bond according to the series method. The k(n) parameter varies as follows: 3(2)→6(3)→9(4)→12(5)→15(6)→18(7)→21(8)→24(9)→27(10)→30(11)→33(12)→36(13). These correspond to the capping series: 4n+2{C⁰C[M-2]}→C¹C[M-2]→C²C[M-2]→C³C[M-2]→C⁴C[M-2]→C⁵C[M-2]→C⁶C[M-2]→C⁷C[M-2]→C⁸C[M-2]→C⁹C[M-2]→C¹⁰C[M-2]→C¹¹C[M-2]. According to the series method, the capping series vary by Δk = 3 and Δn = 1. When the [M-2] capping series are superimposed onto the geometrical framework proposed by Pivoriūnas (Pivoriūnas, 2005) sketched in D-2, then we get the cluster symmetries as

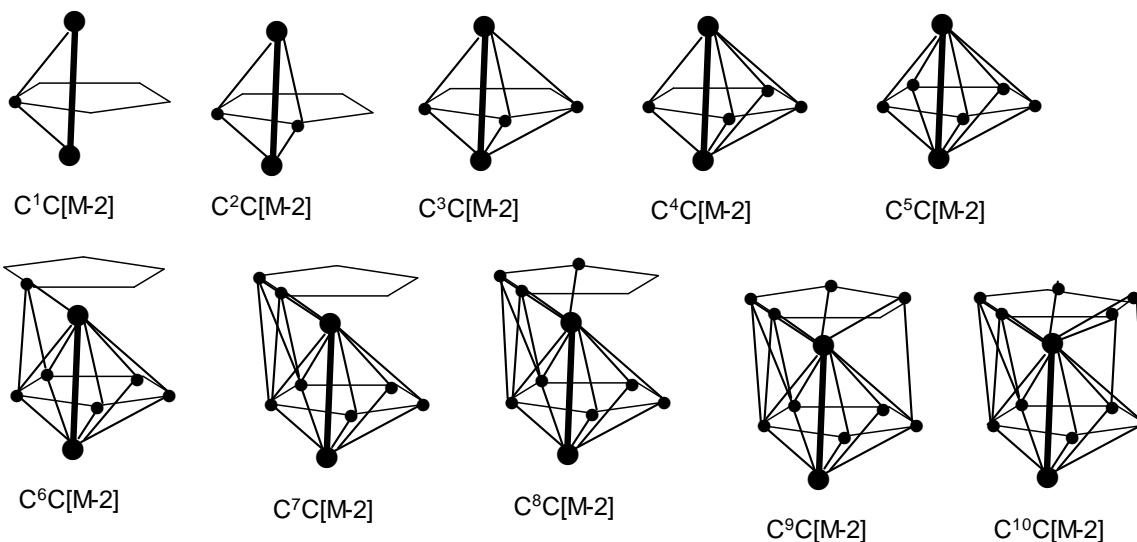
sketched in D-3. What is interesting is that the derived symmetries agree very well with what is observed in the [M-2] based golden clusters. Some of these shapes have been described as being SPHERICALLY CENTERED (Mingos, 1984) as visualized in D-1. We very much know that simple transition metal complexes have a tendency take up specific geometries. For instance, ML_2 (linear), ML_3 (trigonal planar), ML_4 (tetrahedral/square planar), ML_5 (trigonal bipyramid/square pyramid), ML_6 (octahedral) and so on. Similarly, we can apply series method in combination with the Pivoriūnas geometrical model to readily provide a tentative prediction of shapes for golden clusters $C^1C[M-2]$ to $C^{11}C[M-2]$.

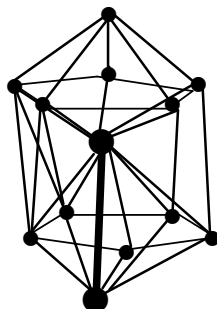


D-1



D-2. Geometric framework for generating observed shapes of [M-2] based golden clusters





D-3. Sketch Illustrating The Formation of [M-2] Based Golden Capped Clusters

3. Conclusion

The series method has successfully been found to categorize the golden clusters and assist in predicting some of their ideal symmetries. This is reflected in the cases of a large number of [M-2] based golden clusters. In this regard, a combination of the [M-2] capping series with the Pivoriūnas geometrical framework has been extremely useful.

Acknowledgement

The author wishes to acknowledge the University of Namibia for financial support and providing the enabling environment, NAMSOV, Namibia for financial assistance and Merab Kambamu Kiremire for proof-reading the draft.

References

- Cotton, F. A., & Wilkinson, G. (1980). *Advanced Inorganic Chemistry, 4th Ed.*, John Wiley and Sons, New York, 1980
- Gimeno, M. C. (2008). *Modern Supramolecular Gold-Metal Interactive and Applications*. Edited A. Laguna, 2008. Wiley-VCH, Weinheim.
- Greenwood, N. N., & Earnshaw, A. (1998). *Chemistry of the Elements, 2nd Ed.* Butterworth, Oxford.
- Kappen, T. G. M. M., Schlebos, P. P. J., Bour, J. J., Bosman, W. P., Smits, J. M. M., Beurskens, P. T., & Steggerda, J. J. (1995a). Synthesis and Characterization of Platinum-Gold Clusters Fused to Tetrahedral Copper Units. *J. Am. Chem. Soc.*, *117*, 8327-8334. <https://doi.org/10.1021/ja00137a005>
- Kappen, T. G. M. M., Schlebos, P. P. J., Bour, J. J., Bosman, W. P., Smits, J. M. M., Beurskens, P. T., & Steggerda, J. J. (1995b). Cluster Growth: Some Representative Reactions. *Inorg. Chem.*, *34*, 2121-2132. <https://doi.org/10.1021/ic00112a027>
- Kilmartin, J. (2010). *Molecular Gold Clusters as Precursors to Heterogeneous Catalysis*. PhD Thesis.
- Kiremire, E. M. R. (2016a). The Application of the 4n Series Method to Categorize Metalloboranes. *Int. J. Chem.*, *8*(3), 62-73. <https://doi.org/10.5539/ijc.v8n3p62>
- Kiremire, E. M. R. (2016b). Clusters of Gold Containing P-Block Elements. *Am. J. Chem.*, *6*(5), 126-144.
- Kiremire, E. M. R. (2016c). A Hypothetical Model for the Formation of Transition metal Carbonyl Clusters Based Upon 4n Series Skeletal Numbers. *Int. J. Chem.*, *8*(4), 78-110. <https://doi.org/10.5539/ijc.v8n4p78>
- Kiremire, E. M. R. (2017). The Golden Series and Clusters of Gold-unique Shapes and Bonding. *Int. J. Chem.*, *9*(1), 38-57. <https://doi.org/10.5539/ijc.v9n1p38>
- Konishi, K. (2014). Phosphine-Coordinated Pure-Gold Clusters and Unique Optical Properties /Responses. *Structure and Bonding*, *161*, 49-86. https://doi.org/10.1007/430_2014_143
- Kwok-Ming, L. (2011). Synthesis, characterization and photophysical properties of Chalcogenido, phosphinidene and alkyl Complexes of Gold(I) and its Congener and their Supramolecular assembly arising from metal-metal interactions. PhD Thesis.
- Mingos, D. M. P. (1984). Gold Cluster Compounds: Are they materials in miniature? *Gold Bull.*, *17*(1), 5-12. <https://doi.org/10.1007/bf03214670>
- Mingos, D. M. P. (1987). Complementary Spherical Electron Density model for Coordination Compounds. *Pure and Appl. Chem.*, *59*(2), 145-154. <https://doi.org/10.1351/pac198759020145>
- Pauling, L. (1977). Structure of Transition Metal Cluster Compounds: Use of an additional orbital resulting from f, g

- character of spd bond orbitals. *Proc. Natl. Acad. Sci., USA*, 74(12), 5235-5238. <https://doi.org/10.1073/pnas.74.12.5235>
- Pei, Y., Shao, N., Jian, D., & Zeng, X. C. (2011). Hollow Polyhedral Structures in Small Gold-Sulfide Clusters. *J. Am. Chem. Soc.*, 1441-1449. <https://doi.org/10.1021/nn103217z>
- Pivoriūnas, G. (2005). Neuer Goldcluster. PhD Thesis.
- Puls, A. B. (2014). A New Synthesis Concept for Metal Doped Gold Clusters. PhD Thesis.
- Raithby, P. R. (1998). The Build-Up of Bimetallic Transition Metal Clusters. *Platinum Metal Rev.*, 42(4), 146-157.
- Sarip, R. (2013). Gold Molecular Clusters to Nanoparticles: A Bottom-up Approach to Supported Nanoparticles for Heterogeneous Catalysis. PhD Thesis.
- Steigelmann, O., Bissing, P., & Schmidbaur, H. (1993). 1,1,1,1-Tetrakis(trioorganylphosphineaurio(I) ethanium(+) Tetrafluoroborates-Hypercoordinated Species Containing $H_3C-C(AuL)_4^+$ cations. *Z. Naturforsch*, 48b, 72-78.
- Van Der Velden, J. W. A. (1983). Preparation and Properties of Gold Cluster Compounds. PhD Thesis.
- Vincente, Chicote, M. T., Abrisqueta, M. D., Gonnzález-Hererro, & Guerrero, R. (1998). Recent Advances in the Chemistry of Gold(I) Complexes with C-,N-,and S-Donor Ligands. *Gold Bulletin*, 31(3), 83-87. <https://doi.org/10.1007/BF03214767>
- Yuan, Y., Cheng, L., & Yang, J. (2013). Electronic Stability of Phosphine-protected Au₂₀ Nanocluster: Superatomic Bonding. *J. Phy. Chem.*, 117, 13276-13282.

Copyrights

Copyright for this article is retained by the author(s), with first publication rights granted to the journal.

This is an open-access article distributed under the terms and conditions of the Creative Commons Attribution license (<http://creativecommons.org/licenses/by/4.0/>).